TMS Middle East - Mediterranean Materials Congress on Energy and Infrastructure Systems (MEMA 2015)
Edited by: Ibrahim Karaman, Raymundo Arroyave, and Eyad Masad
TMS (The Minerals, Metals & Materials Society), 2015

C-Axis Compression of Magnesium Single Crystals: Multi-Scale Dislocation Dynamics Analyses

Wassim Jaber[1], Mu'tasem Shehadeh[1]

[1]American University of Beirut, Beirut, Lebanon

Keywords: Magnesium, Single Crystals, C-Axis Compression, Dislocation Dynamics

Abstract

Hexagonal-closed packed materials (HCP) materials has attracted interest recently due to their unique physical and mechanical properties. The low density and the high strength to weight ratio of such materials make them excellent candidates to save structural weight and consequently fuel consumption in both automotive and aircraft fields. However, the deformation behavior of HCP metals hasn't been completely understood as prior work still lack a detailed understanding on the activation of slip planes and twinning. In addition, the work-hardening behavior and the effect of temperature and strain rate are not yet well-established. This work aims at investigating the deformation mechanisms in magnesium single crystals using Multiscale Dislocation Dynamics Plasticity (MDDP) model. In particular, we focus on modeling the deformation behavior under c-axis compression loading. Several Simulations have been carried out to study the effect of dislocation mobility dependence on the dislocation character and its consequences on the evolution of the dislocation density, the dislocation microstructure, and the hardening behavior. Preliminary results show that the experimentally observed hardening behavior can be reproduced by using linear interpolation of the mobility such that screw segments are stationary and edge segments are highly mobile.

Introduction

In recent years, HCP materials such as Magnesium (Mg), titanium and their alloys have attracted the attention of many research groups due to their unique physical and mechanical properties. The low density and the relatively high specific strength and stiffness of such materials make them excellent candidates to save structural weight, fuel consumption and consequently CO_2 emissions in both the automotive and aircraft fields. Mg's c/a ratio (1.624) is close to the ideal HCP crystal's ratio of 1.633, which make it a good representative element for research studies on HCP materials. Mg is considered to be highly recyclable, possess good machinability, high damping capacity and low melting temperature [1]. Mg alloys have been also used in electronic and biomedical applications due to their electromagnetic shielding capability and biocompatibility [2]. It has been observed that yielding in compression occurs at a stress level three times less than yielding in tension. Unfortunately, this strong tension-compression asymmetry influences the use of magnesium as a structural member [3].

While most of the investigations of the deformation mechanism in metals have been focused on Face-Centered Cubic (FCC) and Body-Centered Cubic (BCC) structures, little work has been performed on HCP structured materials. Due to their low symmetry, the deformation behavior is much more complicated than that of high symmetry FCC metals. Even though there was an increase in their technological applications recently, many fundamental problems remain open; i.e. the identification of active slip systems, work-hardening behavior and strain rate

dependence. A detailed understanding of the relationship between the microstructure of HCP metals and their mechanical properties such as yielding strength, toughness, and hardening laws, is very crucial in the design of HCP based components.

Slip and twinning emerge as the two main deformation modes in HCP metals. Figure 1 shows the different slip planes that are available for dislocation glide in HCP metals. In magnesium, the basal slip of Burgers vector <a> is known to be the easiest system at all temperatures where the c/a ratio is 1.624. The other potential main slip systems are prismatic <a>, pyramidal I <a> and pyramidal II <c+a>. Twinning systems in the $<11\bar{2}0>$ zone are tensile twinning $\{10\bar{1}2\}$, and compressive twinning $\{10\bar{1}1\}$ and $\{10\bar{1}3\}$, with $\{10\bar{1}2\}$ $<10\bar{1}1>$ being the most common twinning system in HCP metals [3, 4, 5].

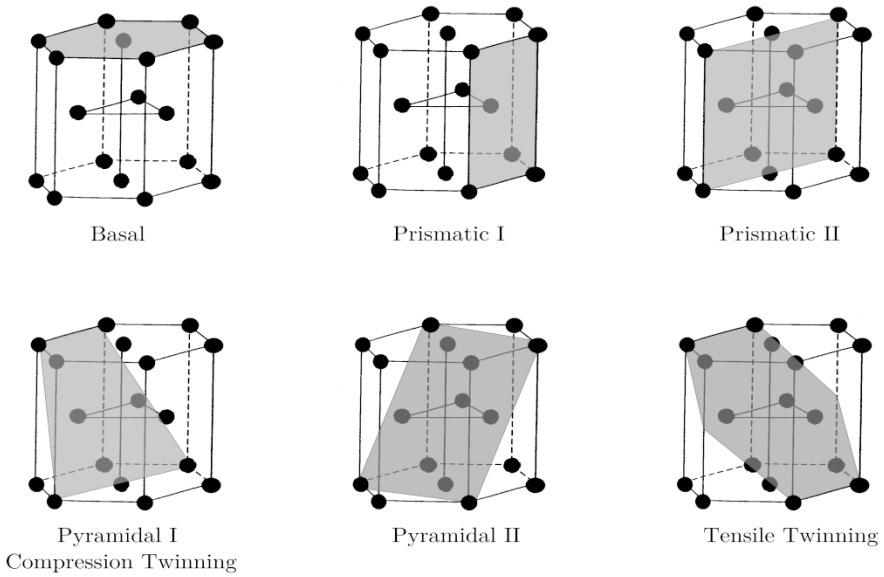

Figure 1: Common Slip and Twinning Planes in HCP

Several experimental studies of the deformation behavior of single-crystal magnesium for c-axis compression and a-axis tension have been carried out. Many studies reported <c+a> pyramidal II slip system as the solo governing deformation mode [5, 6, 7, 8, 9, 10, 11, 12], while other studies observed $\{10\bar{1}1\}$ compression twinning [13, 14, 15], with some reports about the occurrence of both deformation mechanisms [16, 17, 18, 19]. In the early seventies, Obara et al. and Stohr et al. [5, 6] observed pyramidal II slip system for a wide range of temperatures using Transmission Electron Microscopy (TEM) images. However, Chapuis et al. [16] observed that only above 450^{o}C. These contrasting results may be related to the different loading conditions used as Chapuis et al. [16] used channel die compression while Obara et al. [5] used uniaxial compression. The obtained stress-strain curves by Obara et al. [5] showed a strong work hardening rate, especially below 200^{o}C. They suggested that the exhaustion of highly mobile screw dislocations in early stages of deformation is the reason behind the high work-hardening rate. On the other hand, Yoshinga et al. [13] reported basal and prismatic slip acting as accommodation mechanisms for $\{10\bar{1}1\}$ compression twinning. The reported absence of any pyramidal II slip was attributed to the high CRSS of that system compared to lower CRSS of compression twinning. Moreover, pyramidal II slip system is found to be the main operative system below ambient temperature in magnesium-lithium alloy [11].

More recently, Li [17, 18] conducted ambient micro compression loading experiments on magnesium single crystals with their [0001] direction about 10^{o} away from the loading direction. In addition to activation of prismatic <a> and pyramidal II <c+a> slip system, the observed $\{10\bar{1}2\}$ tensile twins refined the sample to become polycrystalline. Non-basal slip force leads to high external stress that may generate crack and result in low ductility. Kim [7] did microcompression tests and observed strong hardening behavior due to the activation and multiplication of <c+a> dislocations on the 6 pyramidal II glide planes. In addition to dislocation interaction, junction formation between <a> and <c+a> dislocations was observed, and are thought to be the reason for hardening. The local misorientation in the sample, resulting from plasticity, activates the basal slip system leading to a massive strain burst [7]. Byer et al., Lilloledin et al. and Syed et al. [8, 9, 19] performed similar tests and reported activation of pyramidal II <c+a> slip system with no deformation twins as observed by [7, 9]. This is in contrast to [19] who suggested that twinning could not be the major form of deformation for this orientation, as the density of twins is low compared to the slip. A-axis tension and c-axis compression of samples were loaded for a wide range of temperatures (77K-573K) by Ando et al. [12]. They observed yielding due to Pyramidal II $\{11\bar{2}2\}$ $<11\bar{2}3>$ slip system, with the yield stress in compression higher than that of tension. In other experiments [14], Plane Strain Compression (PSC) of magnesium single crystals, along the c-axis, resulted in premature failure at very low strain. This observed poor formability was attributed to initial hard orientation and lack of active deformation mechanisms. In the same study, compression along the $<11\bar{2}0>$ and $<10\bar{1}0>$ directions led to activation of $\{10\bar{1}2\}$ extension twinning: The resultant new orientation of the $<11\bar{2}0>$ compression was favorable for basal slip and further $\{10\bar{1}2\}$ twinning, while the second orientation didn't and failed at low strain. The unusually high work-hardening rate present in Mg at ambient c-axis compression is interesting. A possible explanation for such a behavior is in the presence of sessile <c+a> dislocation loops at the basal plane. These loops were previously reported by Stohr et al. [6]. Kumar et al. [20] argued that the mobile screw dislocations intersect other moving screw and stationary edge dislocations, creating jogs that contribute to the work-hardening behavior. Previously, Obara et al. [5] concluded that screw components have higher mobility than edged ones.

In addition to experimental investigations, few simulation approaches has been used to understand the deformation behavior of HCP materials. Monnet et al. [21] performed DD simulations of single crystals zirconium for prismatic glide. DD simulation for titanium was reported by Linder [22]. Kim [7] used DD to simulate deformation behavior of single-crystal magnesium loaded at [0001] orientation in compression. After dislocation multiplication, only 1 or 2 slip planes of the 6 pyramidal 2 slip planes glided intensively, which produced a crystal reorientation, leading to the activation of basal slip. However, Kim [7] was not able to reproduce the hardening behavior observed in experiments. Magnesium single crystals nanopillars were studied using Molecular Dynamics (MD) simulations [23]. The tests were conducted at ambient temperature and high strain rate (10^{6} to 10^{10} s^{-1}). Compression twinning was observed for (0001) loading. MD simulations of c-axis compression in nanoscale magnesium single crystals showed that pyramidal II slip dominates, with no compression twins observed at different temperatures, different loadings and boundary conditions [24]. Gue et al. [24] proposed that the $\{10\bar{1}2\}$ and $\{10\bar{1}1\}$ twins can be activated under c-axis tension, while compression twins will not occur when the c/a ratio of the HCP metal is below $\sqrt{3}$. It is obvious that magnesium single crystal research requires more investigation on both experimental and simulation aspect. Fundamental deformation mechanisms in Mg are subject to discussion, as prior work has often been controversial or inconclusive.

Methodology

Multi-Scale Dislocation Dynamic Plasticity (MDDP)

MDDP is hybrid elasto-viscoplastic simulation model coupling discrete DD with finite element (FE) analysis. DD is used to determine plastic deformation is single crystals by the evaluation of the dislocation evolution history. The dynamic dislocations is governed by a "*Newtonian*" equation of motion, consisting of an inertia term, damping term, and driving force arising from short-range and long-range interactions such that;

$$m_s \dot{\mathrm{v}} + \frac{1}{M_s(T,p)} \mathrm{v} = \mathrm{F}_s \tag{1}$$

Where v is the dislocation velocity, Fs is the Peach Koehler force. The subscript s stands for the segment, m_s is defined as the effective dislocation segment mass density, M_s is the dislocation mobility. The equation of motion is solved to find the velocities and thus the plastic strain rate and the plastic spin are evaluated respectively:

$$\dot{\varepsilon}^{\mathrm{p}} = \sum_{i=1}^{N} \frac{\mathrm{l}_i \mathrm{v}_{\mathrm{gi}}}{2\mathrm{V}} \left(\mathrm{n}_i \otimes \mathrm{b}_i + \mathrm{b}_i \otimes \mathrm{n}_i \right) \tag{2}$$

$$\mathbf{W}^{\mathbf{p}} = \sum_{\mathbf{i=1}}^{\mathbf{N}} \frac{\mathbf{l}_i \mathbf{v}_{\mathbf{gi}}}{\mathbf{2V}} \left(\mathbf{n}_i \otimes \mathbf{b}_i - \mathbf{b}_i \otimes \mathbf{n}_i \right) \tag{3}$$

In the macro level, it is assumed that the material obeys the basic laws of continuum mechanics, i.e. linear momentum balance and energy balance:

$$div\,\mathrm{S} = \rho\, \dot{\mathrm{v}}_p \tag{4}$$

$$\rho\ \mathrm{C_v} \dot{\mathrm{T}} = \mathrm{K} \nabla^2 \mathrm{T} + \mathrm{S}.\dot{\varepsilon}^{\mathrm{p}} \tag{5}$$

Where S is the stress, T is the temperature, v_{p} is the particle velocity, ρ, C_v and K are mass density, specific heat and thermal conductivity respectively. Details of this model are described elsewhere [25, 26, and 27]

Incorporation of HCP Crystallography in MDDP

MDDP framework was originally developed for FCC and BCC materials. In our work here, the framework is modified to accommodate for HCP materials. The commonly used frame of reference to describe slip planes and directions in HCP materials is the hexagonal system. In such system, a slip direction will have a 4 coordinates; this notation is called Miller-Bravias. The four-axis system is based on the a_1, a_2, a_3 and c vectors as shown in Figure 2 below.

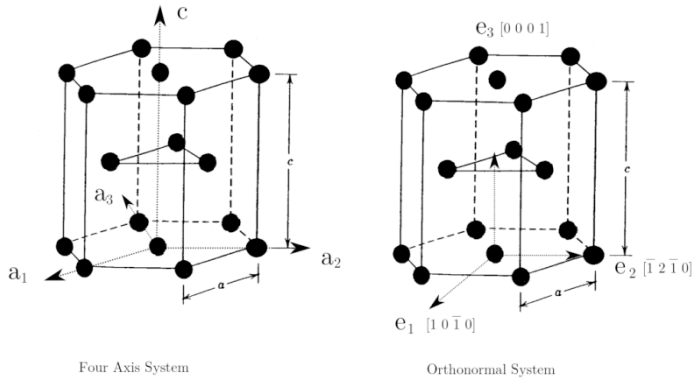

Figure 2: Four-axis system to the left, three-axis orthonormal system to the right

As mentioned earlier, dislocation glide in HCP metals may occur on the basal, prismatic, or pyramidal planes depending on the resolved shear stress on these planes and the their corresponding frictional stresses. Since the MDDP code operates with three-axis orthonormal coordinate system, slip planes and burger vectors are transformed from four-axis Miller-Bravias notation to three-axis orthonormal coordinate system such that unit vector magnitude is equal to a (lattice length). In symmetric crystal structures, slip planes are defined by their respective normal vector having the same indices. However, in Miller-Bravias indices, a direction is not always normal to a plane of the same indices. The transformation from the four-axis plane (hkil) to the normal direction [a_1 a_2 a_3 c] can be expressed as below in equation (6) [3].

$$[a_1\ a_2\ a_3\ c]=\left[\ h\ k\ i\ \left(1.5\times\left(\frac{a}{c}\right)^2\right)l\right] \tag{6}$$

Simulation Setup

The simulation setup (see Figure 4a) is deigned to mimic the uniaxial compression experiment of magnesium single crystals oriented for non-basal directions. The simulation domain has dimensions of 2.5µm×2.5µm×3.2µm (8000b x 8000b x 10000b). To achieve the uniaxial compression loading, a velocity-controlled boundary condition is applied on the upper surface so that a constant strain rate loading is attained. The bottom surface is rigidly fixed while the four sides are kept free. Initially, Frank-Read sources of lengths that range between 0.50µm to 1.0µm are used as agent for dislocation generation. The dislocation sources are randomly distributed on slip planes with a density of about 1.2 * 10^{12} m^{-2}. In DD, periodic boundary condition is used to model dislocation motion in bulk crystals. The simulated sample is set to have anisotropic elasticity. Peierls stress of Pyramidal 2 slip planes is taken as 102 MPa [28]. The material elastic constants and properties used in this work are summarized in tables 1 and 2:

Table 1: Elastic Constants of Mg [29]

Elastic Constant	Value (GPa)
C_{11}	59.7
C_{33}	61.7
C_{44}	16.39
C_{12}	26.2
C_{13}	21.7

Table 2: Material Properties of Mg [3]

Material Property	Value
Density	1740 kg/m^2
Burgers Vector b	3.2 A_0
Poisson's Ratio	0.33
c/a ratio of Mg (at room temperature)	1.623

Two simulation cases are presented here, where we introduced mobility based on dislocation character. Case A has constant mobility values for all dislocations and is taken as base case. Case B has high mobility for edge dislocations, and low mobility for screw ones. Mixed dislocation's mobility is taken as a linear function between edge and screw depending on their orientation.

Table 3: Dislocation Character Motilities for Cases A and B

Cases	Edge Mobility $(Pa.s)^{-1}$	Screw Mobility $(Pa.s)^{-1}$
A	10^5	10^5
B	10^5	0.00001

Results and Discussion

Figure 3 depicts the resulting stress-strain diagrams for the two cases A and B. In case A, the behavior is linear elastic up to 0.45% total strain corresponding to 250 MPa. This large value of the yielding stress is a reflection of the very large frictional stress on the pyramidal-π2 plane (102 MPa), in addition to the stress required to bow-out the dislocation sources. The behavior then assumes a perfect plasticity behavior from 0.5% to 0.7% with no hardening effect. Case B corresponds to the varying mobility case, and the stress-strain curve shows hardening behavior from 0.6 % to 1%. The small fluctuations in the stress-strain curve correspond to the formation and breakage of dipoles. To the best of the authors' knowledge, this result is the first DD simulation to show strong hardening as reported in many experiments. It is worth noting that additional simulations of high mobile screw segments and stationary edge segments have been carried out and showed similar behavior as in case A.

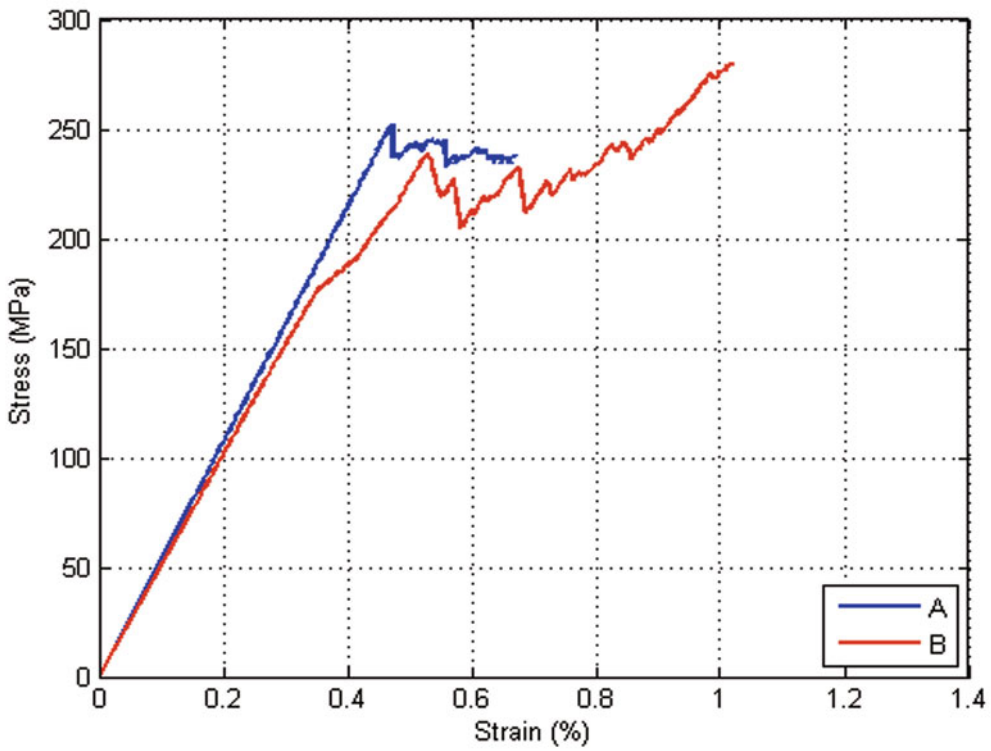

Figure 3: Obtained Stress-Strain Curve for Cases A and B (Best Seen In Colors)

Figure 4 shows snapshots of the dislocation microstructure evolution for case B. As shown in Figure 4(a), numerous dislocation sources are initially placed on the slip planes. As the stress increases, the activation stress for some of the dislocation sources is attained leading to the bow-out of these sources (Figure4(b)) and the increase in the dislocation density. It is worth mentioning that sources placed on the pyramidal planes can only be activated due to fact that in c-compression loading, only pyramidal planes have nonzero Schmid factors (0.45). Additionally, since the screw segments are assumed stationary, we see that pure edge segments sweeps through the crystal at very high speed leaving behind extended dipoles of screw type (see Figure 4(b), (c)). The process continues leading to the accumulation of the dislocation slip on the pyramidal planes in the form of slip bands. Eventually, the simulation domain becomes full of intersecting slip bands with very high dislocation density formed.

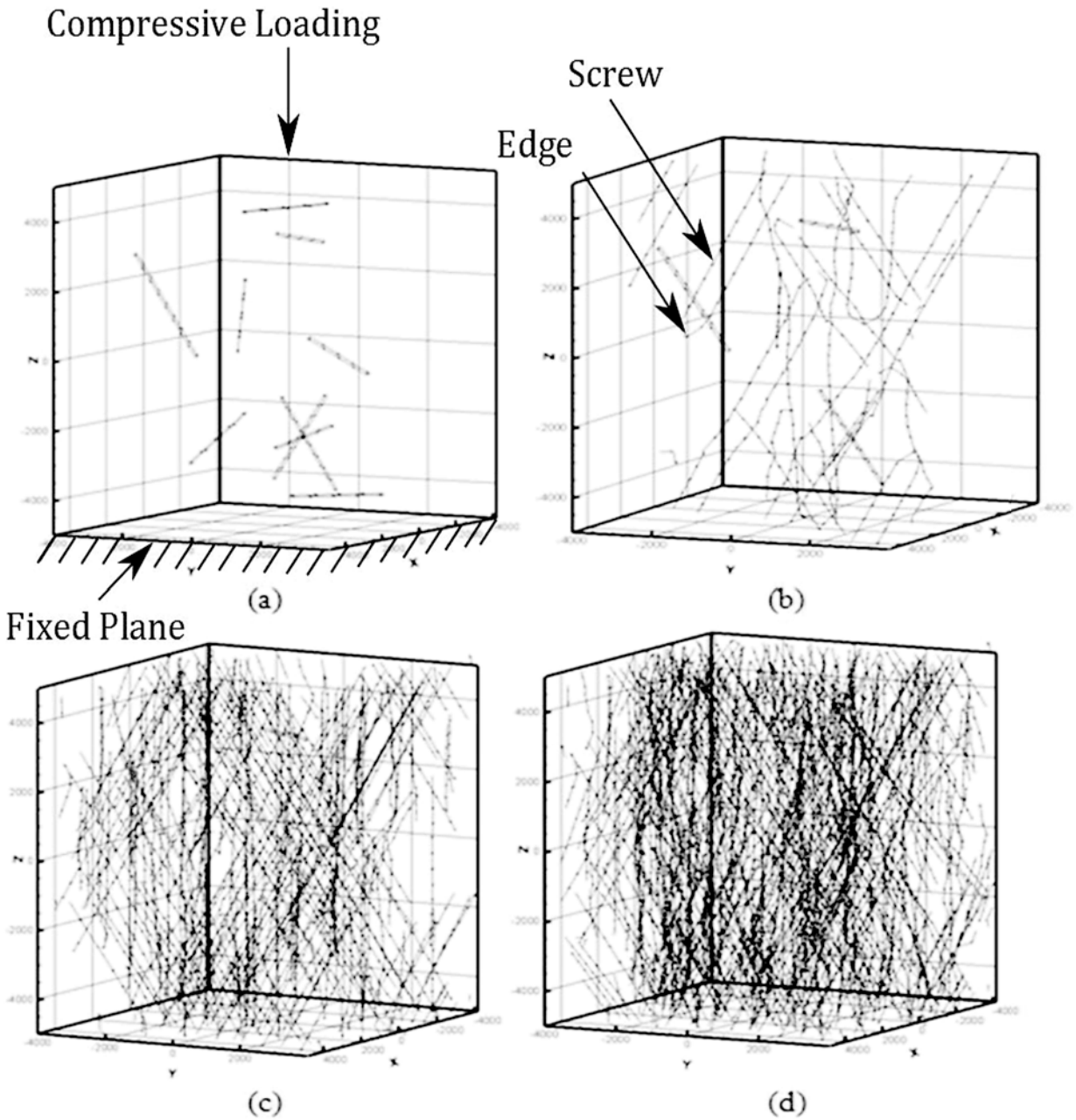

Figure 4: Snapshots of the microstructure evolution in Simulation B. (a) Initial dislocation sources (b) Activation of dislocation sources on pyramidal plane (c) Dislocation glide and activation of new sources (d) Slip bands with dense dislocations are formed

Figure 5 shows the evolution of the dislocation density versus time for case B. Clearly the curve shows three distinct regimes. The first one in which the stress is below the resolved shear stress required to activated the dislocation sources. In that case, dislocations do not move and the dislocation density stays at its initial value of 10^{12} m^{-2}. As the stress increases, the resolved shear stress reach the critical value activates the dislocation sources and abrupt increase in the dislocation density is observed. The process of dislocation emission continues but at a lower rate and eventually dislocation density saturation is attained.

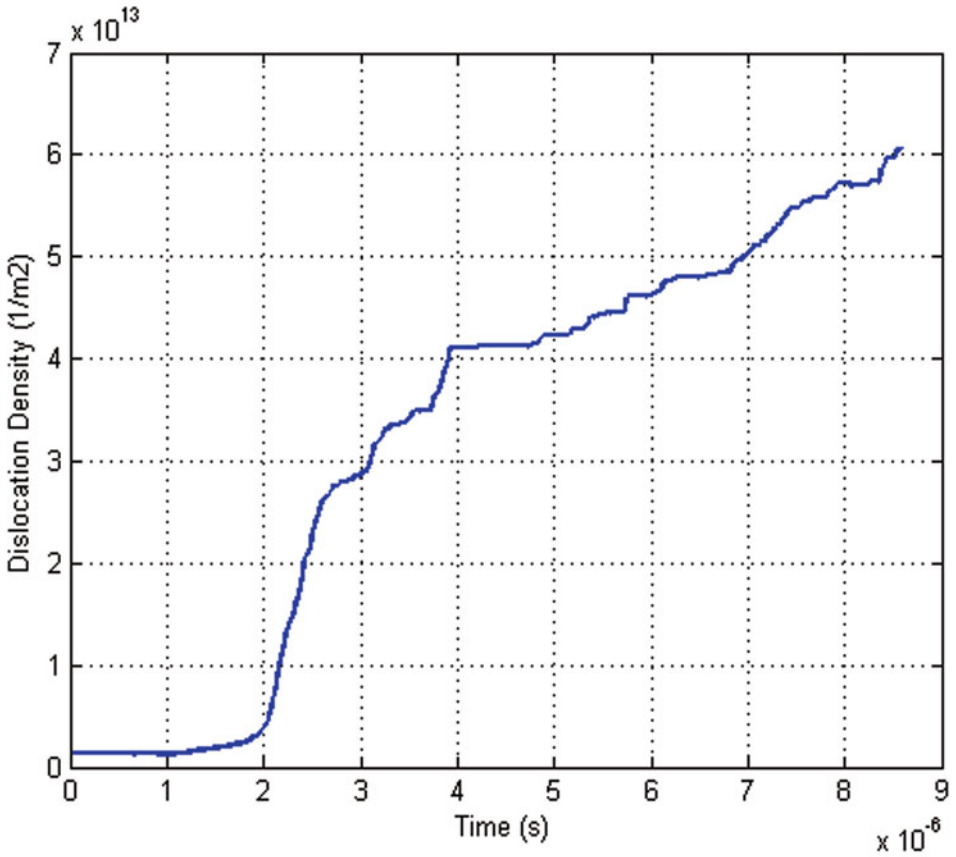

Figure 5: Dislocation Density Increase versus Time

Conclusions

Dislocation dynamics simulations were carried out to study the uniaxial compression of Mg single crystals using MDDP framework. A parametric study for mobility was performed to investigate the consequence of dislocation mobility dependence on dislocation character. We were able to obtain the hardening behavior, observed in experimental studies, by setting a high mobility value to edge segments and the screw dislocations as stationary. These findings provide better understanding of the complicated plastic deformation in hcp crystals, in particular, Mg single crystals under c-axis compression. Recent reports, [30], investigate the effect of Peierls stress as dependent on dislocation orientation. More comprehensive work for Peierls stress variation and its relation to mobility will form future work.

References

[1] Avedesian M, Baker H, editors. ASM specialty handbook, magnesium and magnesium alloys. Materials Park, OH: ASM International;1999.

[2] Li, N., & Zheng, Y. (2013). Novel Magnesium Alloys Developed for Biomedical Application: A Review. Journal of Materials Science & Technology.

[3] Partridge, P. G. (1967). The crystallography and deformation modes of hexagonal close-packed metals. International Materials Reviews, 12(1), 169-194.

[4] Reed-Hill, R.E., Robertson, W.D., 1957. Deformation of magnesium single crystals by nonbasal slip. Transactions of AIME 209, 496-502.

[5] Obara, T., Yoshinga, H., Morozumi, S., 1973. {11-22}<1-1 23> slip systems in magnesium. Acta Metellurgica 21, 845-853.

[6] Stohr, J. F. and J. P. Poirier (1972). "Etude en Microscopie Electronique de Glissement Pyramidal {11-22} <11-23> dans le Magnesium." Philosophy Magzine 25: 1313-1329.

[7] Seok Kim, G. (2011). Small volume investigation of slip and twinning in magnesium single crystals (Doctoral dissertation, Université de Grenoble).

[8] Byer CM., Li B., Cao B., Ramesh KT., Microcompression of single-crystal magnesium, Scripta Mater., 2010:62:536

[9] Lilleodden, E. (2010). Microcompression study of Mg (0001) single crystal. Scripta Materialia, 62(8), 532-535.

[10] Ando S, Nakamura K, Takashima K and Tonda H,1992, J.Japan Inst. of light metals, 42,2845.

[11] Ando, S. and H. Tonda (2000). "Non-Basal Slip in Magnesium-Lithium Alloy Single Crystals." Materials Transactions, JIM 41(9): 1188-1191.

[12] Ando, S., Tsushida, M., & Kitahara, H. (2010, October). Deformation Behavior of Magnesium Single Crystal in c-axis Compression and a-axis Tension. In Materials Science Forum (Vol. 654, pp. 699-702).

[13] Yoshinaga, H., Horiuchi, R., 1963. On the nonbasal slip in magnesium crystals. Trans. Jpn. Inst. Met. 5, 14–21.

[14] Molodov, K. D., Al-Samman, T., Molodov, D. A., & Gottstein, G. (2013). On the Ductility of Magnesium Single Crystals at Ambient Temperature. Metallurgical and Materials Transactions A, 1-7.

[15] B. C. Wonsiewicz and W. A. Backofen: Trans. TMS-AIME, 1967, vol. 239, p. 1422.

[16] Chapuis, A., & Driver, J. H. (2011). Temperature dependency of slip and twinning in plane strain compressed magnesium single crystals. Acta Materialia, 59(5), 1986-1994

[17] Li, Q. (2011). Dynamic mechanical response of magnesium single crystal under compression loading: Experiments, model, and simulations. Journal of Applied Physics, 109(10), 103514.

[18] Li, Q. (2013). Microstructure and deformation mechanism of 0001 magnesium single crystal subjected to quasistatic and high-strain-rate compressive loadings. Materials Science and Engineering: A, 568, 96-101.

[19] Syed, B., Geng, J., Mishra, R. K., & Kumar, K. S. (2012). [0001] Compression response at room temperature of single-crystal magnesium. Scripta Materialia, 67(7), 700-703.

[20] J. Geng, M.F. Chisholm, R.K. Mishra & K.S. Kumar (2014) The structure of ⟨c + a⟩ type dislocation loops in magnesium, Philosophical Magazine Letters, 94:6, 377-386

[21] Monnet, G., Devincre, B., & Kubin, L. P. (2004). Dislocation study of prismatic slip systems and their interactions in hexagonal close packed metals: application to zirconium. Acta materialia, 52(14), 4317-4328.

[22] Linder, T. (2009). Dislocation dynamics simulations.

[23] Luque, A., Ghazisaeidi, M., & Curtin, W. A. (2013). Deformation modes in magnesium (0 0 0 1) and (01$\bar{1}$1) single crystals: simulations versus experiments. Modelling and Simulation in Materials Science and Engineering, 21(4), 045010.
[24] Guo, Y., Tang, X., Wang, Y., Wang, Z., & Yip, S. (2013). Compression deformation mechanisms at the nanoscale in magnesium single crystal. Acta Metallurgica Sinica (English Letters), 26(1), 75-84.
[25] H.M. Zbib and T.D. de la Rubia, Int. J. Plast. 18 (2002) p.1133.
[26] J.P. Hirth, H.M. Zbib and J. Lothe, Model. Simulat. Mater. Sci. Eng. 6 (1998) p.165.
[27] M.A. Shehadeh Phil. Mag. 92 (2012) p.1173.
[28] Staroselsky, A., & Anand, L. (2003). A constitutive model for hcp materials deforming by slip and twinning: application to magnesium alloy AZ31B. *International Journal of Plasticity*, *19*(10), 1843-1864.
[29] Long, T. R., & Smith, C. S. (1957). Single-crystal elastic constants of magnesium and magnesium alloys. Acta Metallurgica, 5(4), 200-207.
[30] Kang, K., Bulatov, V. V., & Cai, W. (2012). Singular orientations and faceted motion of dislocations in body-centered cubic crystals. *Proceedings of the National Academy of Sciences*, *109*(38), 15174-15178.